Resist Heating Dependence on Subfield Scheduling in 50kV Electron Beam Maskmaking

Sergey Babin[†], Andrew B. Kahng[‡], Ion I. Măndoiu[‡], and Swamy Muddu[‡]

[†] Soft Services, 5286 Dunnigan Ct., Castro Valley, CA 94546, USA
[‡] ECE and CSE Departments, University of California at San Diego, La Jolla, CA 92093, USA
sbabin@softsrv.com, {abk,smuddu}@ucsd.edu, mandoiu@cs.ucsd.edu

ABSTRACT

In high-voltage electron beam lithography, most of the beam energy is released as heat and accumulates in the local area of writing. Excessive heat causes changes in resist sensitivity, which in turn causes significant critical dimension (CD) variation. Previous methods for reducing CD distortion caused by resist heating include usage of lower beam currents, increased delays between electron flashes, and multi-pass writing. However, all these methods lower mask writing throughput. This leads to increased mask writing cost, which is increasingly becoming a major limiting factor to semiconductor industry productivity.

In this paper, we propose a new method for minimizing CD distortion caused by resist heating. Our method performs simultaneous optimization of beam current density and subfield writing order. Simulation experiments show that, compared to previous methods, the new subfield scheduling method leads to significant reductions in resist temperature with unchanged mask writing throughput. Alternatively, subfield scheduling can be coupled with the use of higher beam current densities, leading to increased writing throughput without increasing CD distortion.

1. INTRODUCTION

In high-voltage electron beam lithography, most of the beam energy is released as heat and accumulates in the local area of writing. Resist heating has been identified as a main contributor to critical dimension (CD) distortion in high-voltage electron beam maskmaking.[1–4] In an attempt to minimize CD distortion caused by resist heating, recent works[5–8] have explored the optimization of such parameters as beam current density, flash size, number of passes, and subfield writing order. A common drawback of these single-parameter optimizations is that the decreases in resist temperature are obtained at the expense of increasing the mask writing time and cost.

In this paper, we propose a new method for minimizing CD distortion caused by resist heating. Our method performs simultaneous optimization of beam current density and subfield writing order, and is the first to result in decreased resist heating with unchanged mask writing throughput. To reduce excessive resist heating, we schedule the writing of subfields such that successively written subfields are far from each other. To maintain mask writing throughput, we simultaneously increase beam current density so that the resulting reduction in dwell time compensates for the increased travel and settling time caused by non-sequential writing of subfields. Experiments carried out using the commercially available TEMPTA-TION temperature simulation tool[9] show that the new subfield scheduling method leads to significant reductions in resist temperature compared to previous methods. The lower resist temperature enables the use of a higher beam current density. Depending on the particular parameters of the writer, this can reduce total writing time and hence increase throughput while keeping CD distortion within acceptable limits.

The rest of the paper is organized as follows. In Section 2 we describe a subfield scheduling scheme based on the well-spaced labelings of rectangular grids recently introduced by Lagarias,[10] then give a new greedy local improvement subfield scheduling algorithm based on a simple model for computing the temperature of subfields. In Section 3 we present the setup of our simulation experiments comparing the new greedy scheduling with sequential, Lagarias, and random subfield schedules. Finally, in Section 4 we present the results and conclusions.

2. SUBFIELD SCHEDULING ALGORITHMS

One of the most effective techniques for mitigating CD distortion caused by resist heating is to avoid sequential writing of features that are close to each other.[5] When performed at fracture granularity, non-sequential writing greatly increases total mask writing time due to the significant beam re-positioning and settling time overheads. On the other hand, non-sequential writing of subfields incurs much smaller overheads relative to the total mask writing time. Therefore, we concentrate on techniques for improved non-sequential subfield scheduling.

In this section we first review a subfield scheduling method due to Lagarias[5, 10] and then give a new greedy local improvement subfield scheduling algorithm. The Lagarias schedule is based on pure geometric considerations (attempting to maximize the minimum Manhattan distance between consecutively written subfields), whereas the greedy algorithm iteratively improves an initial random schedule by using a simple model for computing the temperature of subfields.

2.1. Lagarias Scheduling

Motivated by applications to error-correction in 2-dimensional memory arrays, Lagarias[10] has recently introduced a class of "well-spaced labeling schemes" for rectangular grids which guarantees that the minimum Manhattan distance between grid nodes with consecutive labels is at most one less than the maximum possible. TEMPTATION simulations results show that Lagarias subfield scheduling can lead to significant reductions in maximum resist temperature compared to the sequential subfield scheduling currently used by electron beam mask writers.[5] However, these results were obtained using constant beam current density, which implies decreased throughput for the Lagarias scheduling due to the beam re-positioning and settling overheads introduced by non-sequential writing of subfields. An interesting open question[5] is whether or not Lagarias scheduling leads to reductions in resist temperature in a normalized throughput setting, i.e., after increasing beam current density such that the resulting reduction in dwell time compensates for the increased travel and settling time in the Lagarias schedule. Simulation results reported in Section 3 answer this question in the affirmative. For completeness, we include here a concise description of the well-spaced labeling scheme of Lagarias.

Let $G(M_1, M_2) = \{(i,j) : 0 \leq i \leq M_1 - 1, 0 \leq j \leq M_2 - 1\}$ be the $M_1 \times M_2$ rectangular grid defined by the subfields. Clearly, we can identify any subfield schedule to a labeling of $G(M_1, M_2)$ with integers from 1 to $M_1 M_2$. An *admissible labeling* of $G(M_1, M_2)$ is a bijection $\phi : [1, M_1 M_2] \longrightarrow G(M_1, M_2)$. The well-spaced labelings of Lagarias are admissible labelings of $G(M_1, M_2)$ defined as follows:

Case 1: M_1 and M_2 are both odd. Set L = least common multiple (l.c.m.) of M_1 and M_2, G = greatest common divisor (g.c.d.) of M_1 and M_2. If $m = iL + j$ with $0 \leq i < G$ and $0 \leq j < L$, then

$$\phi(m) = \left(i + j\left(\frac{M_1 - 1}{2}\right) \pmod{M_1}, \ j\left(\frac{M_2 + 1}{2}\right) \pmod{M_2}\right) \tag{1}$$

Case 2: M_1 is even, M_2 is odd. Then

$$\phi(m) = \left(i + j\frac{M_1}{2} \pmod{M_1}, \ j\left(\frac{M_2 - 1}{2}\right) \pmod{M_2}\right) \tag{2}$$

Case 3: M_1 is odd, M_2 is even. Then

$$\phi(m) = \left(i + j\frac{M_1 - 1}{2} \pmod{M_1}, \ j\left(\frac{M_2}{2}\right) \pmod{M_2}\right) \tag{3}$$

Case 4: M_1 and M_2 are both even. Define

$$L^* = \begin{cases} \frac{1}{2}\text{l.c.m.}(M_1, M_2) & \text{if } \frac{M_1 M_2}{4} \text{ is odd} \\ \text{l.c.m.}(M_1, M_2) & \text{if } \frac{M_1 M_2}{4} \text{ is even} \end{cases} \tag{4}$$

and $G^* = \text{g.c.d.}(M_1, M_2)$. Hence, $M_1 M_2 = H^* G^* L^*$, where

$$H^* = \begin{cases} 2 & \text{if } \frac{M_1 M_2}{4} \text{ is odd} \\ 1 & \text{if } \frac{M_1 M_2}{4} \text{ is even} \end{cases} \tag{5}$$

If

$$m = lG^*L^* + iL^* + j \tag{6}$$

with

$$0 \le j \le L^* - 1; \; 0 \le i \le G^* - 1; \; 0 \le l \le H^* - 1 \tag{7}$$

then

$$\phi(m) = \left(l + j \left(\frac{M_1 - 2}{2} \right) \; (\text{mod } M_1), \; i + j \left(\frac{M_2 - 2}{2} \right) \; (\text{mod } M_2) \right) \tag{8}$$

2.2. The Greedy Local Improvement Algorithm

The main drawback of the Lagarias schedule is its exclusive reliance on geometric considerations. In particular, the schedule is insensitive to travel times between subfields. In this section, we give a greedy algorithm for finding subfield schedules that minimize the temperature experienced by resist. The algorithm is based on the local improvement paradigm, and relies on a simple model that allows fast computation of subfield temperatures. An important feature of the model is that it can take into account travel times between subfields, which usually represents a significant fraction of total writing time.

The greedy algorithm (see Figure 1) starts with a random subfield order, and then iteratively improves the order using a cost function equal to

$$\alpha T_{max} + (1 - \alpha) T_{average} \tag{9}$$

where T_{max} and $T_{average}$ are the maximum, respectively average subfield temperatures for the given order and α is a parameter between 0 and 1 (α was set to 0.5 in our experiments). The algorithm stops when no further decreases in the cost function are possible. As described in Figure 1, the greedy algorithm requires $O(n^2)$ cost function evaluations per each order update. Our implementation reduces the number of cost function evaluations per update to $O(n)$ by considering only swaps (i, j) in which i is a subfield with maximum temperature.

Input: Number of subfields n, mask writer parameters (voltage, current density, travel times, etc.)
Output: Subfield order π

---

1. Generate initial subfield order π uniformly at random

2. Repeat forever

   For all pairs (i, j) of subfields, compute cost of π with i and j swapped

   If there exists at least one cost improving swap, then modify π by applying a swap with highest cost gain

   Else, exit repeat

3. Return subfield order π

Figure 1. The greedy subfield scheduling algorithm

The key part of the greedy algorithm is the evaluation of the cost function (9). Temperature computation based on sophisticated models for electron-beam energy deposition and Green's function integration[11] is impractical even for a relatively small number of subfields. Therefore, we use a greatly simplified model of temperature computation in which each subfield is assumed to be written in a single flash. The model is built on two basic principles: (1) Flashing a subfield within the main deflection field results in increase of temperature at all other subfields, and the increase depends on the distance to the flash, the duration of the flash, the amount of energy deposited by the flash, and the thermal properties of resist. (2) Between flashes, the temperature of all subfields decays exponentially at a rate that depends on the thermal diffusivity of the resist and of the substrate material.[11]

Let $\pi = (\pi_1, \ldots, \pi_n)$ be a flashing order of subfields, and let $T_{i,j}$ be the temperature of subfield π_i before flashing subfield π_j. We assume that $T_{i,1} = 0$ for every $i = 1, \ldots, n$, i.e., the temperature of each subfield before the occurrence

of the first flash is zero. In the time immediately succeeding a flash, the temperature of all other subfields increases by an amount directly proportional to the difference in temperature and inversely proportional to the squared Euclidean distance between them. Let $T_{k,j}^{rise}$ be the temperature rise at subfield π_k due to flashing subfield π_j. $T_{j,j}^{rise}$ is the temperature rise at subfield π_j after being flashed and depends on e-beam writer parameters. For $k \neq j$, $T_{k,j}^{rise}$ is proportional to

$$\frac{T_{j,j} + T_{j,j}^{rise} - T_{k,j}}{dist(\pi_k, \pi_j)^2} \tag{10}$$

where $dist(\pi_k, \pi_j)$ is the Euclidean distance between subfields π_k and π_i.

Finally, an exponential decay in subfield temperature takes place between consecutive flashes. Therefore, the temperature of a subfield π_i before the occurrence of a flash at π_j is

$$T_{i,j} = (T_{i,j-1} + T_{i,j-1}^{rise}) * f \tag{11}$$

where the decay factor f depends on the travel time between flashes.

Based on the above model, all temperatures $T_{i,j}$ can be computed in $O(n^2)$ time. Hence, the cost function (9) can also be evaluated within the same time bound for a given subfield order. This gives a total time of $O(n^4)$ per subfield order update for the greedy algorithm as described in Figure 9. This reduces to $O(n^3)$ for the implementation which considers only candidate swaps involving a subfield with maximum temperature.

3. SIMULATION SETUP AND PARAMETERS

In this section, we describe the experimental setup for thermal simulations of different subfield writing schedules. The commercial TEMPTATION software[9] was used for simulating the thermal evolution of the resist during e-beam exposure. We simulated four scheduling strategies:

1. **Sequential writing schedule**: In this schedule, conventionally used by e-beam writers, writing starts at a corner of the major field and proceeds in a sequential serpentine fashion.

2. **Lagarias writing schedule**: In this schedule, writing is performed according to the order specified by the analytical formulas given in Section 2.1. The Lagarias order for 16×16 subfields is given in Figure 2.

3. **Random writing schedule**: We used the randomly generated order for 16×16 subfields in Figure 3.

4. **Greedy writing schedule**: In this schedule, the writing is performed based on the order computed by the greedy local improvement described in Section 2.2. The order is shown in Figure 4.

We simulated a major field of size $1.024mm \times 1.024mm$, divided into 16×16 subfields of size $64\mu m \times 64\mu m$ each. For each subfield we simulated a chessboard fracture pattern exposed in sequential-serpent order as shown in Figure 5. Mask and e-beam parameters used in our TEMPTATION simulations are given in Table 1.

For each subfield scheduling, the simulation was performed in two phases. In the first simulation phase, each of the 256 subfields was exposed to four coarse flashes that delivered to the subfield the same dose as the detailed chessboard fracture flashes. Furthermore, the four doses were specified such that subfield writing time was identical to that required by detailed chessboard fracture flashes. This coarse simulation captures the effect of subfield scheduling on the *average* subfield temperature before writing.

During first simulation phase, delays were introduced between subfield flashes to simulate the effect of travel and settling time between subfields. In our simulations we assumed a constant settling time of $25ns$ and a travel time proportional to the maximum distance traveled in either the horizontal or vertical direction. More exactly, the settling time was computed using the formula $25ns + 5ns \times \max\{\Delta x, \Delta y\}$, where Δx and Δy are the horizontal and vertical travel distances, respectively. To maintain constant throughput among various subfield writing schedules, we increased the beam current density to reduce the dwell time by an amount equal to the overhead in travel and settling times. The resulting current density values were 20.0 A/cm^2 for sequential, 21.3 A/cm^2 for random, 21.8 A/cm^2 for Lagarias, and 21.5 A/cm^2 for the greedy subfield order.

As a result of first phase simulations we identified for each subfield ordering the subfield with the largest average temperature before writing, which we call "critical" subfield. Detailed fracture flashing was then simulated for each of the four critical subfields corresponding to each ordering.

Plate type	ZEP7000 resist on chrome and glass
Dimensions of main deflection field	$1.024mm \times 1.024mm$
Dimensions of deflection subfield	$64\mu m \times 64\mu m$
#Subfields	256
Flash size	$2\mu m \times 2\mu m$
#Flashes per subfield	512
Flash exposure time	1ns
Accelerating voltage	50kV
Resist sensitivity	$10\mu C/cm^2$

Table 1. Mask and e-beam writer parameters

4. RESULTS AND CONCLUSIONS

Figure 6 shows the temperature before writing for each of the 16×16 subfields under the four considered writing schedules. The greedy, Lagarias and random schedules have a lower average subfield temperature compared to the sequential schedule. The maximum subfield temperature is lower for the greedy schedule than for the Lagarias and random.

Figure 7 shows the temperature before writing for the fractures in the critical subfields corresponding to the four simulated schedules. The results show that the worst fracture temperature before writing for the greedy order is reduced to 93.4°C compared to 105.1°C for sequential, 104.6°C for random, and 97.15°C for Lagarias order. The lower resist temperature enables the use of a higher beam current density. Depending on the particular parameters of the writer, this can reduce total writing time and hence increase throughput while keeping CD distortion within acceptable limits.

REFERENCES

1. N. Kuwahara, H. Nakagawa, M. Kurihara, N. Hayashi, H. Sano, E. Murata, T. Takikawa and S. Noguchi, "Preliminary Evaluation of Proximity and Resist Heating Effects Observed in High Acceleration Voltage E-Beam Writing for 180-nm-and-beyond Rule Reticle Fabrication", *SPIE Symposium on Photomask and X-Ray Mask Technology VI*, SPIE Vol. 3784, 1999, pp. 115-125.
2. C. A. Mack, "Electron Beam Lithography Simulation for Mask Making, Part VI: Comparison of 10 and 50kV GHOST Proximity Effect Correction", *Photomask and Next-Generation Lithography Mask Technology VIII*, SPIE Vol. 4409, 2001, pp. 194-203.
3. K. Nakajima and N. Aizaki, "Calculation of a Proximity Resist Heating in Variably Shaped Electron Beam Lithography", *J. Vac. Sci. Technol. B* 10(6) (1992), pp. 2784-2788.
4. H. Sakurai, T. Abe, M. Itoh, A. Kumagae, H. Anze and I. Higashikawa, "Resist Heating Effect on 50kV EB Mask Writing", *SPIE Symposium on Photomask and X-Ray Mask Technology VI*, SPIE Vol. 3748, 1999, pp. 126-136.
5. S.V. Babin, A.B. Kahng, I.I. Mandoiu, and S. Muddu, "Subfield scheduling for throughput maximization in electron-beam photomask fabrication," *Emerging Lithographic Technologies VII*, R.L. Engelstad (ed.), Proc. SPIE #5037, 2003, to appear.
6. S. Babin and I. Kuzmin, "Throughput optimization of electron beam lithography in photomask fabrication regarding acceptable accuracy of critical dimensions", *21st Annual BACUS Symposium on Photomask Technology*, Proc. SPIE, Vol. 4562, 2002, pp. 545-551. 16, 1998, 3241.
7. K. Kikuchi, H. Ohnuma and H. Kawahira, "New Optimization Method of the Exposure with Alternative Phase Shifting Masks", *Photomask and Next-Generation Lithography Mask Technology VIII*, SPIE Vol. 4409, 2001, pp. 41-51.
8. Lee H. Veneklasen, "Optimizing Electron Beam Lithography Writing Strategy Subject to Electron, Optical, Pattern, and Resist Constraints", *J. Vac. Sci. Technol. B* 9(6) 1991, pp. 3063-3069.
9. Sergey Babin, Igor Yu. Kuzmin, "Experimental Verification of the TEMPTATION (temperature simulation) software tool", *J. Vac. Sci. Technol B* 16(6), 1998, pp. 3241-3247.
10. J.C. Lagarias, "Well-Spaced Labelings of Points in Rectangular Grids", *SIAM Journal of Discrete Math*, 13(4), 2000, pp 521-534.
11. I.Y. Kuzmin, "Simulation of resist heating using TEMPTATION software with different models of electron-beam energy deposition", *Emerging Lithographic Technologies III*, SPIE Vol. 3676, 1999, pp. 536-542.

1	17	33	49	65	81	97	113	129	145	161	177	193	209	225	241
248	8	24	40	56	72	88	104	120	136	152	168	184	200	216	232
239	255	15	31	47	63	79	95	111	127	143	159	175	191	207	223
214	230	246	6	22	38	54	70	86	102	118	134	150	166	182	198
205	221	237	253	13	29	45	61	77	93	109	125	141	157	173	189
180	196	212	228	244	4	20	36	52	68	84	100	116	132	148	164
171	187	203	219	235	251	11	27	43	59	75	91	107	123	139	155
146	162	178	194	210	226	242	2	18	34	50	66	82	98	114	130
137	153	169	185	201	217	233	249	9	25	41	57	73	89	105	121
128	144	160	176	192	208	224	240	256	16	32	48	64	80	96	112
103	119	135	151	167	183	199	215	231	247	7	23	39	55	71	87
94	110	126	142	158	174	190	206	222	238	254	14	30	46	62	78
69	85	101	117	133	149	165	181	197	213	229	245	5	21	37	53
60	76	92	108	124	140	156	172	188	204	220	236	252	12	28	44
35	51	67	83	99	115	131	147	163	179	195	211	227	243	3	19
26	42	58	74	90	106	122	138	154	170	186	202	218	234	250	10

Figure 2. Subfield writing sequence for 16×16 Lagarias scheduling

137	131	44	171	130	35	256	124	127	83	149	12	126	195	242	138
14	244	246	170	132	231	77	214	104	207	107	40	163	26	84	229
5	10	70	36	199	56	112	224	220	230	3	205	174	31	45	247
48	18	219	129	59	216	19	147	33	227	122	52	64	102	254	218
118	71	11	200	49	148	140	68	32	146	46	206	198	213	97	164
186	187	156	73	179	6	136	17	42	160	240	1	234	67	177	61
99	90	23	226	53	94	155	217	141	9	135	4	192	75	108	211
43	39	72	204	248	7	212	91	100	54	62	183	167	63	145	223
115	29	66	20	173	188	125	117	197	222	110	25	34	92	235	41
139	89	233	243	252	255	28	185	251	151	55	27	215	22	182	237
194	121	158	103	86	180	95	58	47	16	13	101	81	57	178	60
193	133	79	88	245	98	175	37	253	24	69	74	114	161	80	93
176	172	51	78	105	157	196	113	241	96	191	109	225	144	128	111
166	152	228	15	116	208	154	169	21	168	250	238	232	201	203	153
209	120	30	236	76	239	106	65	50	82	162	123	249	2	134	221
159	8	85	142	143	181	119	202	87	150	165	189	184	38	210	190

Figure 3. Subfield writing sequence for 16×16 random schedule

1	178	239	44	205	180	110	146	40	128	103	175	107	60	76	26
17	119	56	157	221	99	8	162	25	69	235	81	196	158	210	42
31	105	213	246	120	138	47	218	243	203	135	22	222	92	182	58
49	91	187	6	94	228	251	194	89	176	151	244	117	149	11	74
65	240	72	150	66	168	36	73	127	50	32	67	2	46	230	90
190	24	200	38	108	209	57	169	160	208	183	101	255	140	195	106
97	229	171	54	181	142	19	83	226	16	85	133	165	18	219	122
113	156	13	125	28	164	115	43	249	144	116	206	247	45	236	14
129	184	253	86	197	234	216	5	104	256	231	152	30	188	77	154
145	79	61	4	153	102	132	71	174	23	199	51	109	88	7	170
161	237	215	118	245	204	35	192	63	126	95	254	137	220	37	186
177	29	93	15	80	223	9	82	217	48	33	163	12	173	124	202
193	134	70	41	141	59	167	252	185	114	224	78	191	143	227	3
147	20	111	166	27	212	123	98	233	139	55	242	211	62	96	131
225	84	207	52	100	148	75	39	201	172	21	198	136	232	179	250
241	34	68	238	189	64	155	130	248	112	87	121	53	159	214	10

Figure 4. Subfield writing sequence for 16×16 Greedy scheduling
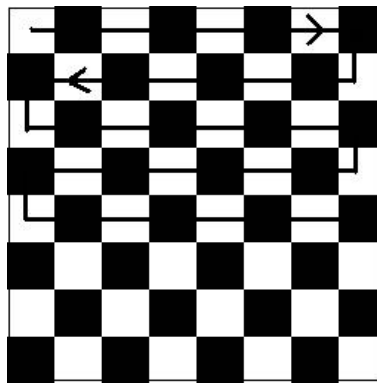
Figure 5. Flash exposure pattern inside a subfield
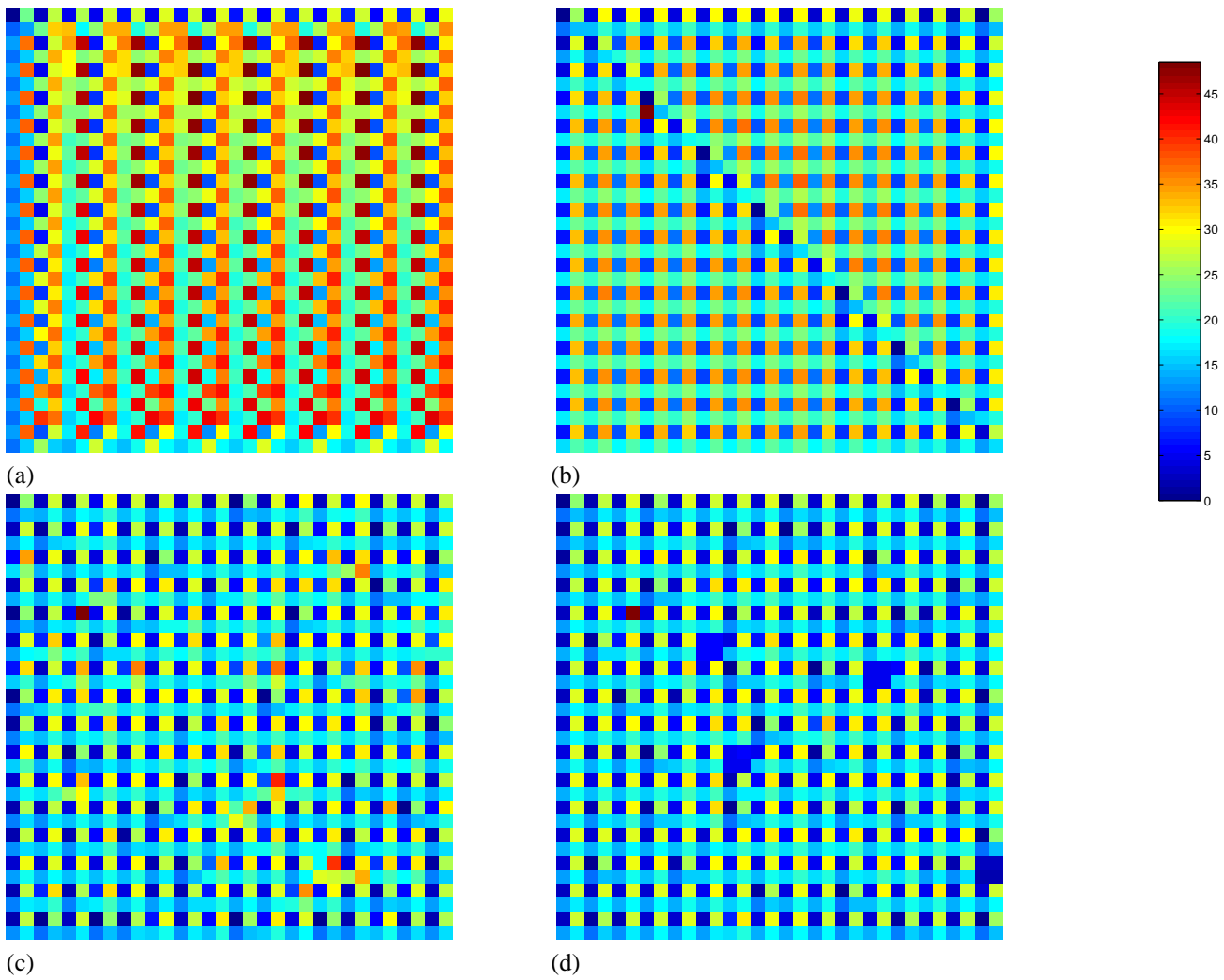
Figure 6. Thermal profile of 16×16 subfields for four writing schedules: (a) sequential, (b) Lagarias, (c) random, and (d) greedy. The color code shown is used for all writing schedules.
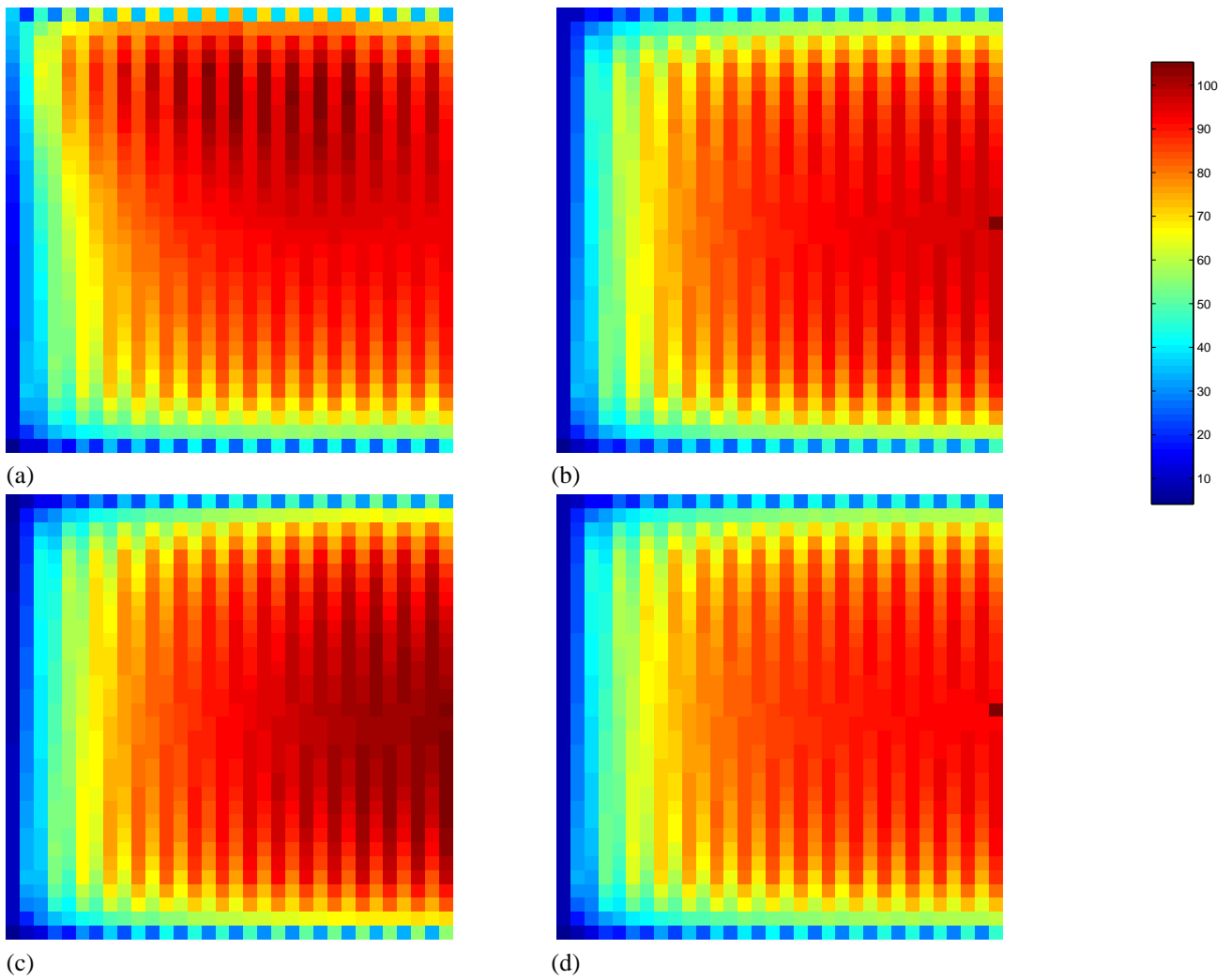
Figure 7. Thermal profile of the critical subfield (the subfield with maximum temperature) for four writing schedules: (a) sequential, (b) Lagarias, (c) random, and (d) greedy. The color code shown is used for all writing schedules.